

RESIDUAL STRENGTH PREDICTION FOR MULTI-DIRECTIONAL COMPOSITES SUBJECTED TO ARBITRARY FATIGUE LOADS

Marc Möller¹, Jochen Blaurock², Gerhard Ziegmann³ and Alfons Esderts⁴

^{1*} TH Köln, Institute for Automotive Engineering,
Betzdorfer Str. 2, Cologne, Germany,
marc.moeller@th-koeln.de, <https://www.th-koeln.de/>

² TH Köln, Institute for Automotive Engineering,
Betzdorfer Str. 2, Cologne, Germany,
jochen.blaurock@th-koeln.de, <https://www.th-koeln.de/>

³ TU Clausthal, Institute of Polymer Materials and Plastics Engineering,
Agricolastr. 6, Clausthal-Zellerfeld, Germany,
ziegmann@puk.tu-clausthal.de, <https://www.puk.tu-clausthal.de/>

⁴ TU Clausthal, Institute for Plant Engineering and Fatigue Analysis,
Leibnizstr. 32, Clausthal-Zellerfeld, Germany,
alfons.esderts@imab.tu-clausthal.de, <https://www.imab.tu-clausthal.de/>

Key words: Fatigue, Residual Strength, Multi-directional Laminates, Ply-wise Modeling

Abstract. As it is important to know a structures capacity of carrying further loads after particular load or time periods, a in-depth investigation on the computation of residual strength of multi-directional laminates is presented in this paper. The computational model focuses on ply-wise structural analysis of continuous fibre reinforced plastics at the mesoscale level and thus it belongs to the group of mechanistic models. The aim of the paper is to determine the fatigue life and residual strength of multi-directional laminates with the exclusive use of uni-directional ply data. For this reason, detailed strength degradation at the ply level is considered and the application of suitable models for the lifetime and residual strength estimation after certain combined fatigue loads is examined. Results for laminates under pulsating and alternating stress ratios for the different models are discussed in terms of their benefits and limitations for a practicable application. It is finally shown, that the nonlinear models are a great improvement for residual strength calculation and agree very well with experimental data from well documented composite fatigue data base OptiDAT.

1 INTRODUCTION

The use of composite materials for various structural parts rises strongly due to their excellent ratio of high strength and stiffness to low weight. Almost all of those parts are

subjected to cyclic loads in the course of their operating lifetimes. Therefore, there is a strong demand in covering new and optimized computation capabilities concerning the fatigue of composite materials. To predict fatigue life of multi-directional fibre reinforced plastics under cyclic loads with the exclusive use of data from uni-directional tests, a computational tool for structural analysis is developed. Beside the calculation of fatigue life itself, it also is essential to know the laminates capacity of carrying further loads after a defined load history. Therefore, different residual strength models are examined in a subsequent static analysis. Philippidis and Passipoularidis carried out a detailed examination of various residual strength models with focus on probabilistic and deterministic theories in 2007 [1]. The main finding was that no model was able to predict the residual strength degradation behavior of varying multi-directional composites. Their results showed, that the use of more complicated models, which require a lot of parameters and therefore large experimental data, did not necessarily improve the description of the residual strength behavior of laminates. For the mechanistic approach in this study, some of the examined deterministic residual strength models are used for the description of known residual strength characteristics at the uni-directional ply-level. Within the next steps, the unknown residual strength of multi-directional laminates is calculated via structural analysis.

2 FLOW CHART

The tool for the lifetime estimation of composites is based on iterative layerwise structural analysis per load cycle and degradation of stiffness and strength on the ply-level as shown in figure 1. A subsequent residual strength calculation of the laminate is following

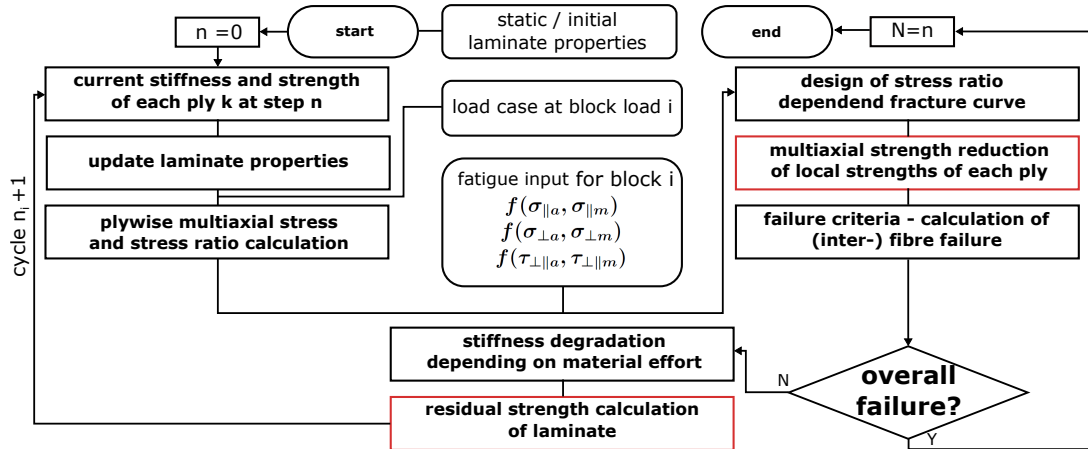


Figure 1: Flow chart for the lifetime and residual strength estimation

the plywise analysis. The figure shows a simplified flow chart with the main focus of the present work highlighted in red. The Puck failure theory [2] is used for prediction of matrix and fibre failure at the ply-level.

3 THEORY OF RESIDUAL STRENGTH MODELS

As mentioned before, Philippidis and Passipoularidis [1] examined a lot of probabilistic and deterministic residual strength models. Two of the examined deterministic models, the linear model by Broutman and Sahu [3] and the nonlinear model used by Reifsnider et al. [5] and Schaff et al. [4], as well as one recently published model by Stojkovic et al. [6] are selected for closer examinations in this work. Reasons for the selection of these models are for example the satisfaction of the fracture condition at the end of fatigue life, the dependency upon the endured number of cycles and a reasonable amount of required parameters compared to other models.

3.1 Linear model

In 1972, Broutman and Sahu [3] published a model, which decreases residual strength linearly with the ratio of endured cycles to maximum number of cycles at the specific stress amplitude. Strength degradation starts with the initial strength and should generally satisfy the fracture condition $S(n = N) = \sigma_{max}$ at the last step. The linear model is described by

$$S_r = S_{st} - (S_{st} - \sigma_{max,i}) \left(\frac{n_i}{N_i} \right) \quad (1)$$

where S_r is the residual strength after a specific number of endured cycles n_i , S_{st} is the static initial strength, $\sigma_{max,i}$ is the maximum stress at the actual step and N_i is the maximum allowed number of cycles for the actual stress $\sigma_{max,i}$ derived from experimental S-N curves. The linear residual strength model is one of the most widely used theories, because it doesn't need any fitting of parameters and it is well known for giving conservative results on the safe side. Since the maximum number of cycles is needed, the only necessary input is a extrapolated S-N-curve at the specific stress ratio.

3.2 Nonlinear model

The nonlinear model was used by Reifsnider et al. in 1986 [5] and Schaff and Davidson in 1997 [4]. In this case, the linear model is extended with an additional parameter to account for nonlinear material behavior. Equation (1) is then modified to

$$S_r = S_{st} - (S_{st} - \sigma_{max,i}) \left(\frac{n_i}{N_i} \right)^\alpha \quad (2)$$

including the parameter α , which controls the shape of the nonlinear function. The strength degradation is then described with either a steep loss of strength at the beginning ($\alpha < 1$) or at the end ($\alpha > 1$) of the laminate lifetime.

3.3 Normalized Strength Reserve Model

In 2017, Stojkovic, Folic and Pasternak [6] published a improved model, called the Normalized Strength Reserve Model (NRSRM). Basically the model is the expansion of the nonlinear model with an additional parameter β . The normalized strength reserve $S_{res,n}$

is defined as

$$S_{res,n} = \left(1 - \left(\frac{n}{N}\right)^\alpha\right)^\beta \quad (3)$$

with the additional parameter β , which controls the shape of the function in conjunction with parameter α . The residual strength is then calculated by

$$S_r = \sigma_{max,i} + (S_{st} - \sigma_{max,i})(S_{res,n}) \quad (4)$$

The parameters α and β can either be obtained by fitting normalized strength reserve data, wherein strength reserve is the difference between residual and maximum strength, to equation (3) or the residual strength data directly to equation (4), which is similar to the other models. The advantage of the NRSM model is that the typical initial loss of strength followed by slow degradation as well as the sudden decrease in strength at the end can be modeled very well.

3.4 Implemented routine

The models described in section 3.1 - 3.3 are brought together to one procedure for the application within the computational routine. For a iterative computation, the drop of strength in every step is defined by

$$S_{r,i} = S_{r,i-1} - \Delta S_{r,i} \quad (5)$$

where $S_{r,i}$ and $S_{r,i-1}$ are the residual strengths at the actual and last step respectively and $\Delta S_{r,i}$ is the drop of residual strength in the i-th cycle and is calculated from

$$\Delta S_{r,i} = \left\{ \left[(S_{st} - \sigma_{max,i}) \left(1 - \left(\frac{n_{i-1}}{N_i}\right)^{\alpha_i}\right)^{\beta_i} \right] - \left[(S_{st} - \sigma_{max,i}) \left(1 - \left(\frac{n_i}{N_i}\right)^{\alpha_i}\right)^{\beta_i} \right] \right\} \quad (6)$$

Herein, for simulations on the ply-level, the strengths $S_{r,i}$, $S_{r,i-1}$ and S_{st} represent the five local strengths at the ply-level in terms of the parallel tensile and compressive strengths (X_t , X_c), the transverse tensile and compressive strengths (Y_t , Y_c) or the in-plane shear strength ($S_{\perp\parallel}$). According to that, the maximum stress $\sigma_{max,i}$ represents the corresponding stresses $\sigma_{\parallel max}$, $\sigma_{\perp max}$ or $\tau_{\perp\parallel max}$ respectively.

4 EXPERIMENTAL DATA

Fatigue data from experimental tests is taken from the OptiDAT¹ database [7]. All of the evaluated laminates are glass fibre reinforced plastics (GFRP). The uni-directional

¹The OPTIMAT BLADES project is a European research project, supported by the European Union. Project Coordinators: Wind Turbine Materials and Constructions (WMC, Netherlands) and Energy Research Centre of Netherlands (ECN - Netherlands). Database Contributors: Center for Renewable Energy Sources (CRES - Greece), German Aerospace Center (DLR - Germany), Rutherford Appleton Laboratory (RAL - United Kingdoms), National Research Laboratory (RISOE - Denmark), University of Patras (UP - Greece), Technical Research Center (VTT - Finland), Free University Brussels (VUB - Belgium) and Wind Turbine Materials and Constructions (WMC - Netherlands).

material consists of non-woven unidirectional glass rovings with a minor amount of off-axis reinforcement, made of polyester (PES) yarn, and the biaxial material consists of non-woven glass rovings in 2 layers ($\pm 45^\circ$). The dry fibers are infused with the epoxy system “Prime 20” by vacuum assisted resin transfer molding and the system is post-cured at 80°C for 4 hours [8].

Mat.#1 The first examined material configuration is the uni-directional laminate with stacking sequence $[0]_5$ from OptiDAT database [7], named “UD2”.

Mat.#2 Transverse tested uni-directional laminate with stacking sequence $[0]_7$ from OptiDAT database [7], named “UD3”.

Mat.#3 Biaxial laminate with stacking sequence $[\pm 45]_5$ from OptiDAT database [7], named “MD3”.

Mat.#4 Multi-directional laminate with stacking sequence $[(\pm 45/0)_4/\pm 45]$ from OptiDAT database [7], named “MD2”.

5 INPUT FROM STATIC AND FATIGUE MATERIAL TESTS

As illustrated in figure 1, there are mainly three types of input data needed for the calculations: values from static and fatigue tests, as well as static tests after specific fatigue loads. Only input data for static and fatigue tests of uni-directional (Mat.#1 and Mat.#2) and biaxial (Mat.#3) specimen is used as input data. Table 1 shows the static input values, which are used to calculate the initial condition of the multi-directional laminate. The values are derived from static tests of flat specimen made from Mat.#1-3, which consist of fibre volume content between 51,94 % and 53,73 %.

	E_{\parallel}	E_{\perp}	$G_{\perp\parallel}$	$\nu_{\perp\parallel}$	R_{\parallel}^+	R_{\parallel}^-	R_{\perp}^+	R_{\perp}^-	$R_{\perp\parallel}$
	GPa	GPa	GPa		MPa	MPa	MPa	MPa	MPa
mean value	38,43	14,07	4,23	0,2893	810,56	469,96	55,88	164,95	56,1

Table 1: Calculated static values for experimental data from [7]

S-N curves at pulsating tensile ($R=0.1$), pulsating compressive ($R=10$) and alternating stress ($R=-1$) ratios of each material Mat.#1-3 were used as input data for fatigue life and residual strength calculations within the model.

Data for residual strength formulation of all five local strengths X_t , X_c , Y_t , Y_c or $S_{\perp\parallel}$ at the ply-level is used for a deeper investigation on multiaxial fatigue. Figure 2 shows the fit of equations (1), (2) and (3) to experimental data of Mat.#1 for different stress ratios and stress amplitudes. Figure 2a illustrates the fitted curves for experimental residual strength data plotted against the fractional life n/N . The strength reserve for the NRSM is also shown in the upper right corner of Figure 2a. As can be seen Figure 2b and 2c,

there is no degradation of compressive strength modeled in fibre direction under pulsating

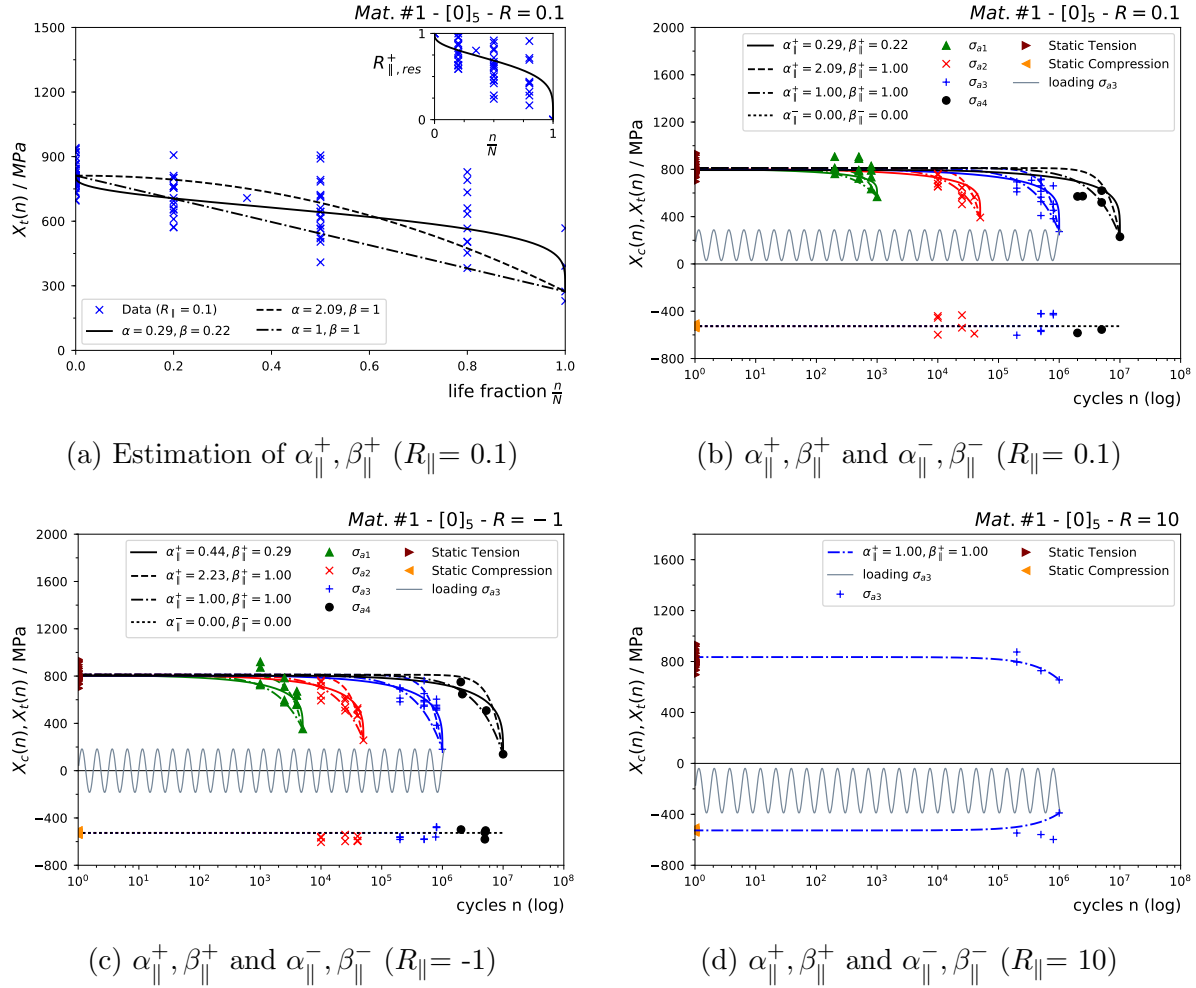
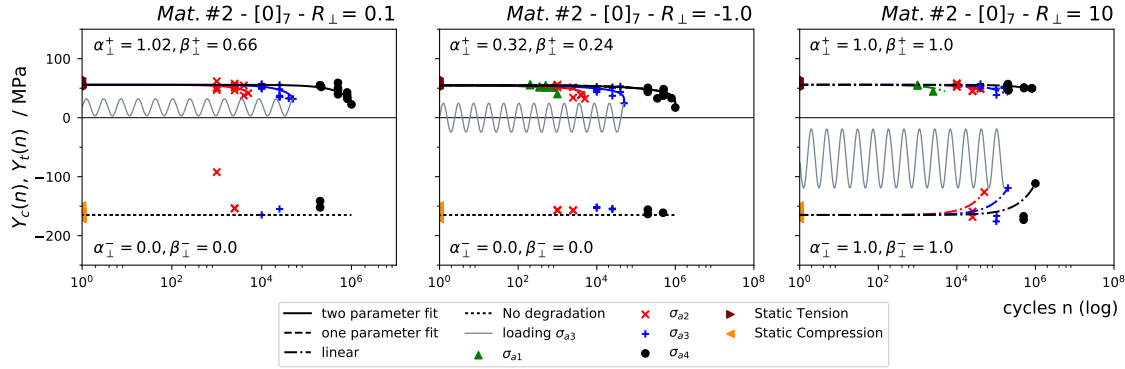


Figure 2: Estimation of parameters α_{\parallel}^+ , β_{\parallel}^+ and α_{\parallel}^- , β_{\parallel}^- for various stress ratios and arbitrary stress amplitudes with the use of experimental data for Mat.#1.

tensile and alternating stress ratios. Furthermore, only linear degradation of tensile and compressive strength is modeled under pulsating compression stress ratios as shown in Figure 2d. Figure 3 shows a similar behavior in compressive strengths under pulsating tensile and alternating stress ratios for transverse loaded Mat.#2. Transverse tensile and compressive strengths are modeled with linear degradation under pulsating compression stresses in the same way as for parallel strengths. Shear strength is only fitted with data from pulsating tensile stress tests and consequently the same parameters are used for any stress ratio.

In the present paper, three varying combinations of parameters are examined. The first setup ‘‘Rconfig.#1’’ is based on linear strength degradation of all five strengths values. The second setup ‘‘Rconfig.#2’’ is based on the use of equations (1) and (2) and the last


 Figure 3: Estimation of parameters $\alpha_{\perp}^+, \beta_{\perp}^+$ and $\alpha_{\perp}^-, \beta_{\perp}^-$ for Mat.#2.

setup ‘‘Rconfig.#3’’ makes use of (1) and (3). For a better overview of the investigated configurations, the combinations of parameter α and β are compiled in Table 2.

	Rconfig. #1	Rconfig. #2	Rconfig. #3	unvaried
	$\alpha_{\parallel}^+, \beta_{\parallel}^+$	$\alpha_{\parallel}^+, \beta_{\parallel}^+$	$\alpha_{\parallel}^+, \beta_{\parallel}^+$	$\alpha_{\parallel}^-, \beta_{\parallel}^-$
$R = 0.1$	1.00, 1.00	2.09, 1.00	0.29, 0.22	0.00, 0.00
$R = -1$	1.00, 1.00	2.23, 1.00	0.44, 0.29	0.00, 0.00
$R = 10$	1.00, 1.00	1.00, 1.00	1.00, 1.00	1.00, 1.00
	$\alpha_{\perp}^+, \beta_{\perp}^+$	$\alpha_{\perp}^+, \beta_{\perp}^+$	$\alpha_{\perp}^-, \beta_{\perp}^-$	$\alpha_{\perp}^-, \beta_{\perp}^-$
$R = 0.1$	1.00, 1.00	1.49, 1.00	1.02, 0.66	0.00, 0.00
$R = -1$	1.00, 1.00	1.22, 1.00	0.32, 0.24	0.00, 0.00
$R = 10$	1.00, 1.00	1.00, 1.00	1.00, 1.00	1.00, 1.00
	$\alpha_{\perp\parallel}, \beta_{\perp\parallel}$	$\alpha_{\perp\parallel}, \beta_{\perp\parallel}$	$\alpha_{\perp\parallel}, \beta_{\perp\parallel}$	
any ratio	1.00, 1.00	1.89, 1.00	0.70, 0.37	

Table 2: Coefficients for residual strength simulation with experimental data from [7]

6 STIFFNESS DEGRADATION

The type and size of stiffness degradation at the ply level has an influence on the fatigue life and residual strength of multi-directional laminates due to stress redistribution within the plies. For this reason, a closer examination of the stiffness reduction is carried out in the first place. Within the model, the stiffness is reduced as follows [9, 10]:

$$E_{\perp}(n) = E_{\perp}^0 \left(\frac{1 - \eta_{r,\perp}}{1 + c_{\perp}(f_{e,IFF}(n) - 1)^{\xi_{\perp}}} + \eta_{r,\perp} \right) \quad (7)$$

$$G_{\perp\parallel}(n) = G_{\perp\parallel}^0 \left(\frac{1 - \eta_{r,\perp\parallel}}{1 + c_{\perp\parallel}(f_{e,IFF}(n) - 1)^{\xi_{\perp\parallel}}} + \eta_{r,\perp\parallel} \right) \quad (8)$$

where E_{\perp}^0 and $G_{\perp\parallel}^0$ are the initial transverse and shear stiffness and $E_{\perp}(n)$ and $G_{\perp\parallel}(n)$ are the transverse and shear stiffness at the current cycle n . The parameter $\eta_{r,\perp}$ and $\eta_{r,\perp\parallel}$ represent the residual stiffness value at higher values of inter-fibre-failure and $c_{\perp\parallel}$, $\xi_{\perp\parallel}$ and c_{\perp} , ξ_{\perp} are mainly controlling the shape of the degradation function. As shown in Table 3, six varying combinations of stiffness degradation parameters are analyzed. The combination of parameters in configuration ‘‘Sconfig.#1-#4 focus on transverse stiffness and the configurations ‘‘Sconfig.#5-#6’’ focus on shear stiffness degradation.

Sconfig.	#1	#2	#3	#4	#5	#6
$\eta_{\perp}(\eta_{\perp\parallel})$	0.30 (0.25)	0.50 (0.25)	0.03 (0.25)	0.30 (0.25)	0.30 (0.10)	0.30 (0.50)
$\xi_{\perp}(\xi_{\perp\parallel})$	1.31 (1.50)	1.31 (1.50)	1.31 (1.50)	1.50 (1.50)	1.31 (1.50)	1.31 (1.50)
$c_{\perp}(c_{\perp\parallel})$	5.34 (0.70)	5.34 (0.70)	5.34 (0.70)	0.70 (0.70)	5.34 (0.70)	5.34 (0.70)

Table 3: Coefficients for stiffness degradation

7 RESULTS AND DISCUSSION

Due to the influence of stiffness degradation on the stress redistribution within multi-directional laminates, the dependency of residual strength calculation on the stiffness parameters is investigated in the first step. Figure 4 exemplarily shows the residual strength calculation under pulsating tensile stress ratio $R=0.1$ with a constant global amplitude load $\hat{\sigma}_a = 116.4$ MPa for multi-directional laminate Mat.#4. The influence of the varied parameters is shown for each residual strength setup from Table 2.

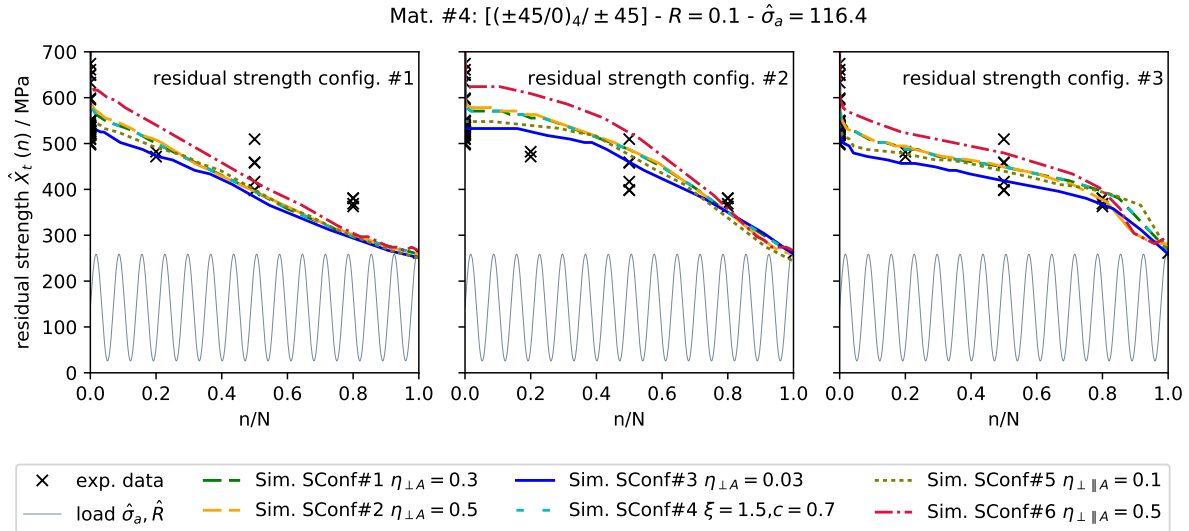


Figure 4: Simulated stiffness degradation for different residual strength configurations under stress ratio $R=0.1$ with constant amplitude $\hat{\sigma}_a = 116.4$ MPa for Mat.#4

As can be seen in the figures above, the influence of varied stiffness parameters on residual strength curves is very similar in all three configurations. First of all, while there is no big difference in the curves for $\eta_{\perp A} = 0.3$ (Sconf.#1) and $\eta_{\perp A} = 0.5$ (Sconf.#2), the choice of lower $\eta_{\perp A}$ (Sconf.#3) leads to the most conservative predictions. Of course, the result is due to higher stress redistribution into less damaged plies, which will lead to earlier failure and lower residual strength predictions respectively. The same effect can be observed for varied shear modulus parameter $\eta_{\perp\parallel A} = 0.1$ (Sconf.#5) and $\eta_{\perp\parallel A} = 0.5$ (Sconf.#6). Although, $\eta_{\perp\parallel A}$ does have a higher significance in the investigated multi-directional laminate with stacking sequence $[(\pm 45/0)_4/\pm 45]$ and higher values (as in Sconf.#4) will lead to conservative predictions of fatigue life and residual strength. At the same time, the predictions for faster degradation ($\xi = 1.5$ and $c = 0.7$) with relation to inter-fibre failure (Sconf.#4) has nearly no effect on the calculation of residual strength. That is because of the rapid growth of inter-fibre failure in the $\pm 45^\circ$ plies during the first cycles at high stress amplitudes. In the following, Sconf.#1 is chosen for stiffness degradation under inter-fibre failure mode A and Sconf.#2 is used for degradation under inter-fibre failure mode B and C for all further investigations:

- $\eta_{\perp A} = 0.3$ and $\eta_{\perp B,C} = 0.5$
- $\xi_{\perp A,B,C} = 1.31$, $c_{\perp A,B,C} = 5.34$ and $\eta_{\perp\parallel A,B,C} = 0.25$, $\xi_{\perp\parallel A,B,C} = 1.5$, $c_{\perp\parallel A,B,C} = 0.7$

Figure 5 shows the simulation results for Mat.#4 under pulsating tensile stress for different stress amplitudes. The results of global tensile strength \hat{X}_t are captured very accurately

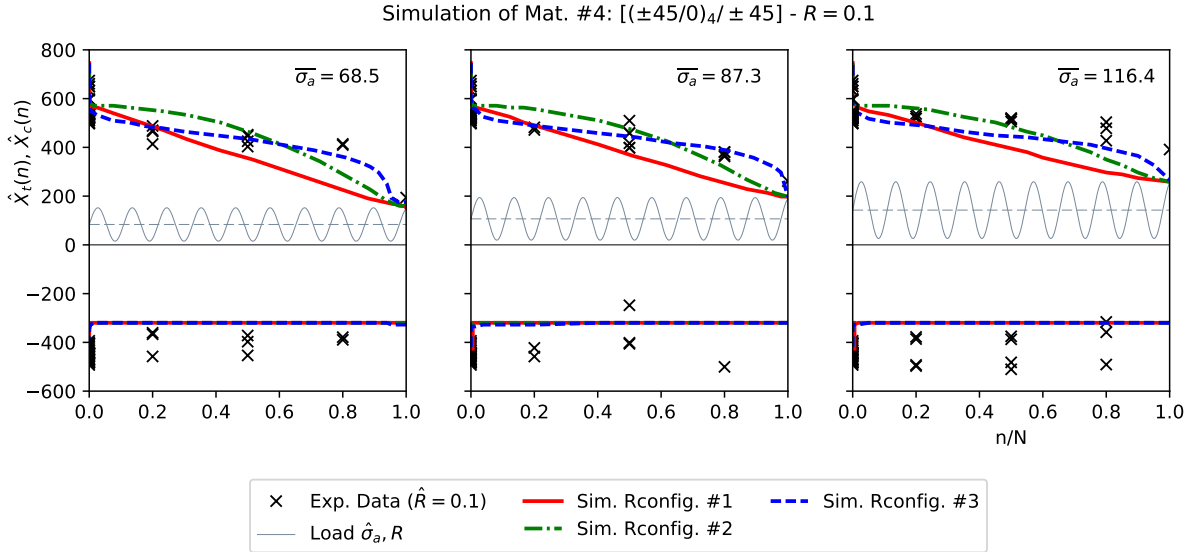


Figure 5: Residual strength estimation for Mat.#4 under pulsating tensile stress and different stress amplitudes

with the use of Rconfig.#3. The three main stages in terms of the loss of tensile strength at the beginning, a widely constant level during a lot of cycles and the drop of strength

during the last number of cycles are depicted precisely. While Rconfig.#1 is predicting residual tensile strength until a life fraction of $\sim 20\%$, it is extremely conservative for the rest of the lifetime. Rconfig.#2 tends to overestimate residual tensile strength at lower cycles on the one hand and to underestimate it at higher cycles on the other hand. The model tends to generally underestimate residual compressive strength with any of the examined configurations. While the static compressive strength \hat{X}_c is calculated very accurately, there is a steep drop in strength after the first few cycles due to stiffness degradation after inter-fibre failure mode A. From the authors point of view, part of the reason for this is that the micro-scale effect of contacting crack edges, which will lead to crack-closure and therefore higher stiffness under compressive loads, is not recognized within the ply-wise model. Figure 6 illustrates the results for Mat.#4 under varying alternating stresses. The predictions of residual strength are very similar to the previous cases shown in Figure 5. Both of the nonlinear configurations tend to overestimate residual

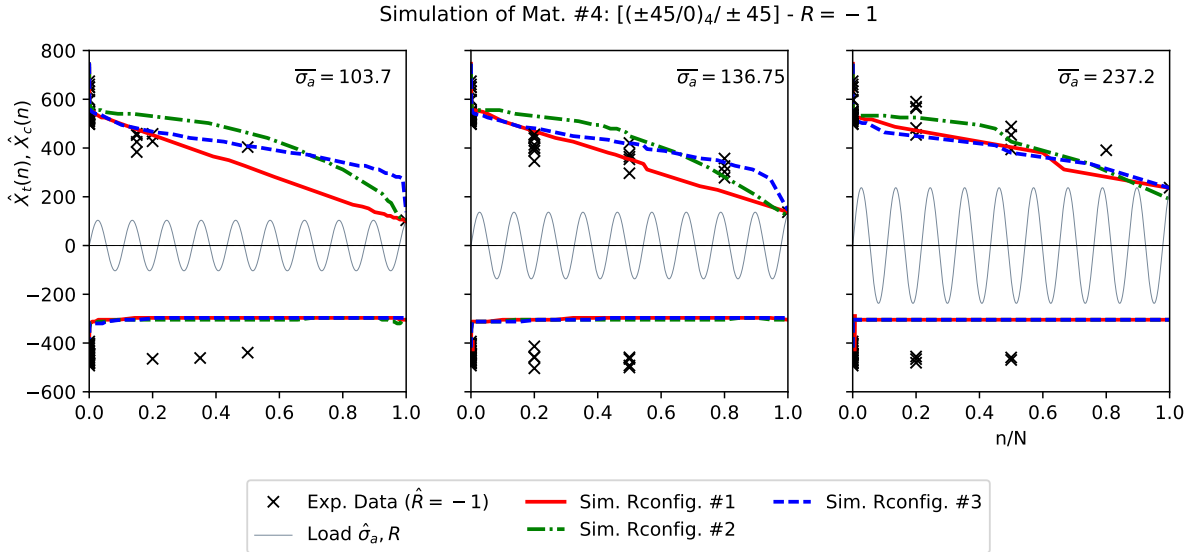


Figure 6: Residual strength estimation for Mat.#4 under alternating stress and different stress amplitudes

tensile strength \hat{X}_t at the lower stress amplitudes $\hat{\sigma}_a = 103.7$ MPa and 136.75 MPa over a wide range of cycles, as can be seen in the left and middle figure. The results at higher stress amplitudes in the right figure are captured very well by all of the three configurations. In this case, the residual compressive strength \hat{X}_c is also underestimated by the model due to the same effect mentioned above. Figure 7 shows the results for Mat.#4 under pulsating compressive stress with different stress amplitudes. Since the reduction in strength is unvaried for simulation under compressive stress ratios and only the linear model is used within the analysis, all of the models predict the same residual strength behavior. As can be seen in the graph, the predictions for residual tensile strength \hat{X}_t are very good compared to the residual strength data for life fractions beneath $\sim 30\%$. For higher number of cycles, the predictions are on the safe side. Concerning the residual

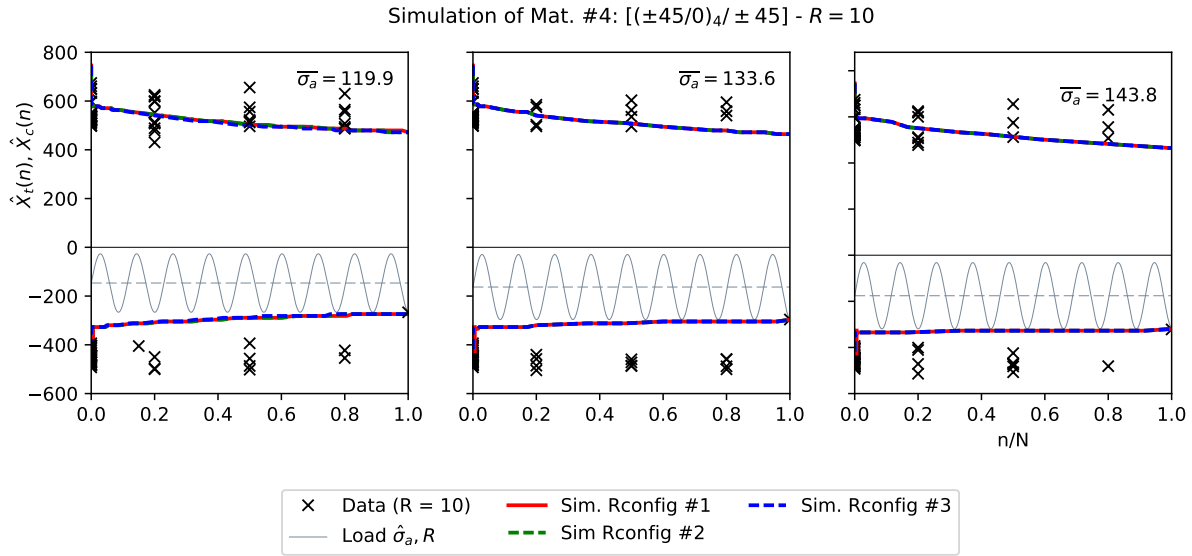


Figure 7: Residual strength estimation for Mat.#4 under pulsating compressive stress and different stress amplitudes

compressive strength \hat{X}_c , the predictions are subject to the same cause mentioned in the results for pulsating tension and alternating stress ratios above. This shows very well, that further analysis and investigations concerning the compression strength is necessary.

8 Conclusion and future work

In conclusion, it can be stated that the use of nonlinear residual strength models within the multiaxial approach improves the predictions of residual tensile strength \hat{X}_t for pulsating tensile and alternating stress ratios. Residual compressive strength \hat{X}_c was underestimated for each stress ratio and therefore gave too conservative results. Compared to the linear model, the disadvantage is the higher amount of experimental data needed to fit parameters α and β . Nevertheless, the significantly better prediction of residual strengths at higher number of cycles is a huge advantage. Still the findings leave questions for the future, which will be addressed in forthcoming works:

- a deeper investigation on improvements for the residual compressive strength under arbitrary stress ratios will be carried out
- the model will be further developed for fatigue life and residual strength predictions under variable amplitude loads

REFERENCES

- [1] T.P. Philippidis and V.A. Passipoularidis: *Residual strength after fatigue in composites: Theory vs. experiment*. International Journal of Fatigue, Vol. 29, pp. 2104-2116, 2007, doi:<https://doi.org/10.1016/j.ijfatigue.2007.01.019>.

- [2] A. Puck and H. Schrmann: *Failure analysis of FRP laminates by means of physically based phenomenological models*. Composites Science and Technology, Vol. 62, pp. 1633-1662, 2002, [https://doi.org/10.1016/S0266-3538\(01\)00208-1](https://doi.org/10.1016/S0266-3538(01)00208-1).
- [3] L. Broutman and S. Sahu: *A new theory to predict cumulative fatigue damage in fiberglass reinforced plastics*. Composite Materials: Testing and Design (2nd Conference), ASTM STP497, Corten HT (1972) 170188. DOI:10.1520/STP27746S.
- [4] J. R. Schaff and B. D. Davidson: *Life prediction methodology for composite structures. part i - constant amplitude and twostress level fatigue*. Journal of Composite Materials (1997) 170188. DOI:10.1177/002199839703100202.
- [5] K. Reifsnider and W.W. Stinchcomb: *A critical-element model of the residual strength and life of fatigue-loaded composite coupons*. Composite Materials: Fatigue and Fracture K.L., ASTM STP-907, American Society for Testing and Materials, Philadelphia, PA (1986), pp. 298-313
- [6] N. Stojkovic and F. Radomir and H. Pasternak: *Mathematical model for the prediction of strength degradation of composites subjected to constant amplitude fatigue*. International Journal of Fatigue(2017) 478487. DOI:<https://doi.org/10.1016/j.ijfatigue.2017.06.032>.
- [7] R. Nijssen: *Optidat - fatigue of wind turbine materials database*. Available at https://wmc.eu/optimatblades_optidat.php.
- [8] T. K. Jacobsen: *Material Specification, Reference Material (OPTIMAT) - Glass-epoxy material*. Optimat Blades, Material Specification, Doc. No: 10004, revision 1, May 7th, 2002.
- [9] A. Puck and M. Mannigel: *Physically based non-linear stress-strain relations for the inter-fibre fracture analysis of FRP laminates*. Composites Science and Technology, vol. 67, pp. 1955 - 1964, 2007.
- [10] S. Adden and P. Horst: *Stiffness degradation under fatigue in multiaxially loaded non-crimped-fabrics*. International Journal of Fatigue, vol. 32, pp. 108–122, 2010.